

Fermi National Accelerator Laboratory

FERMILAB-Conf-93/337-E

CDF

CDF Results on Electroweak Physics

**Henry J. Frisch
For the CDF Collaboration**

*The Enrico Fermi Institute and Physics Department, University of Chicago
Chicago, Illinois*

*Fermi National Accelerator Laboratory
P.O. Box 500, Batavia, Illinois 60510*

November 1993

*Presented at the International Conference on Elastic and Diffractive Scattering, Vth Blois Workshop,
Brown University, Providence, Rhode Island, June 8-12, 1993*

Beyond Run Ib the schedule fluctuates wildly. Both D0 and CDF have substantial upgrades in progress, driven partly by the increased luminosity and by a change in the bunch spacing from 3.5 microseconds to 132 nanoseconds. These changes require substantial changes in the CDF calorimeters and front-end and trigger electronics, as well as increased capability in tracking. Budget limitations for these (modest) upgrades to the two detectors may mean that the world's highest energy accelerator can not run in 1995, and the schedule for completion of the detector upgrades is uncertain.

2 W and Z production, R, and the W width

The measured cross-sections times branching ratio for W and Z production are shown in Figure 3 versus \sqrt{s} [3, 4]. Also shown are theoretical predictions using the MRS D'_0 and D'_- parton distribution functions [5]. The agreement is quite good, although the predictions now sit slightly high compared to the data. For fun, also shown are the theoretical predictions from 1985 [6], showing how the situation has changed from that time, when the predictions were quite low with respect to the measurements. The changes have been: 1) the measured value of the W mass has gone down from 83 GeV to 80 GeV [7], leading to an increase of approximately 10% in the predicted cross-section; 2) the branching ratio for $W^\pm \rightarrow e^\pm \nu$ has changed from approximately 1/12 to 1/9 as we now know from the CDF limit that the top quark channel is closed to the W decay as long as the top decays according to the Standard Model; 3) the cross-sections can now be calculated to NNLO; 4) the parton distribution functions have increased at low values of x; and 5) the charm contribution has increased. The limitation in the cross-section measurement is now the uncertainty in the determination of the luminosity.

One can extract the width of the W, Γ_W , from the ratio of the W and Z cross-sections times branching ratios, using the method of Cabibbo [8] and Halzen and Mursula [9]. The idea is to compare the ratio of observed $W^\pm \rightarrow e^\pm \nu$ decays to observed $Z^0 \rightarrow e^+ e^-$ decays. The ratio, R , can be expressed as:

$$R = \frac{\sigma(W \rightarrow e\nu)}{\sigma(Z^0 \rightarrow e^+e^-)} = \frac{\sigma(\bar{p}p \rightarrow WX)}{\sigma(\bar{p}p \rightarrow Z^0X)} \frac{\Gamma(W \rightarrow e\nu)}{\Gamma(Z^0 \rightarrow e^+e^-)} \frac{\Gamma(Z^0)}{\Gamma(W)}. \quad (1)$$

From R , either the ratio of total widths $\Gamma(Z^0)/\Gamma(W)$ or the branching ratio for W into electrons can be extracted with the predicted value for the ratio of production cross sections, the measured partial and total widths of the Z^0 , and the predicted partial widths of the W .

The analysis is based on the same principle as our previous analyses of R [4, 10]: we select a 'good' electron in the central detector where the electron identification is very robust, and then select both the W and Z samples as subsets of this inclusive central electron sample. In this method both the W and Z samples share the common first electron leg, and consequently many of the systematic uncertainties involving

electron identification efficiencies and trigger efficiencies cancel. The inclusive sample is selected with electron identification cuts that differ only very slightly from the cuts in our previous publications[11]. Figure 4 shows the E_T spectrum of inclusive electrons at this stage of selection. The Jacobian peak from the W and the Z is prominent.

From the inclusive sample W candidates are selected by an additional single requirement, that there be greater than 20 GeV of missing E_T in the event. We select Z candidates by requiring a second electromagnetic isolated cluster in the event which makes an invariant mass with the first electron in the range $65 \text{ GeV}/c^2 < M_{ee} < 115 \text{ GeV}/c^2$. In addition both W and Z events are required to have the event vertex within 60 cm of the interaction point along the beam (z) direction. In 18.4 pb^{-1} there are 30507 inclusive central electrons, 10991 $W^\pm \rightarrow e^\pm \nu$ candidates, and 1053 $Z^0 \rightarrow e^+e^-$ candidates. Of the Z^0 candidates, 41% are central-central, 49% are central-plug, and 10% are central-forward [12]. The transverse mass spectrum for the W candidates is shown in Figure 5; the invariant mass spectrum for the Z candidates is shown in Figure 6.

The W and Z samples are corrected for background, acceptance, and lepton identification efficiency. The corrections are listed in the table of Figure 7. We note only that both the acceptances and the efficiencies for the W and Z are very similar, with $A_W/A_Z = 0.908 \pm 0.015$, and $\epsilon_W/\epsilon_Z = 1.025 \pm 0.012$. The backgrounds in this preliminary analysis will be reduced in the final analysis.

The preliminary result for R is:

$$R = 10.65 \pm 0.36(\text{stat.}) \pm 0.27(\text{sys.}). \quad (2)$$

We emphasize that the number is preliminary; more work is being done on the background subtractions, the acceptances and the efficiencies. In addition, the last few pb^{-1} of data are being added to the data set.

Using a predicted value for the ratio of the W and Z production cross-sections $\sigma(\bar{p}p \rightarrow WX)/\sigma(\bar{p}p \rightarrow Z^0X) = 3.33 \pm 0.03$ [13], and the theoretical value for $\frac{\Gamma(W \rightarrow e\nu)}{\Gamma(Z^0 \rightarrow e^+e^-)}$ of 2.696 ± 0.018 [14], we find:

$$\frac{\Gamma(Z^0)}{\Gamma(W)} = 0.819 \pm 0.033 \quad (3)$$

Using the LEP value for $\Gamma(Z^0)$ of $2.492 \pm 0.007 \text{ GeV}$ [15] we then find

$$\Gamma(W) = 2.033 \pm 0.069(\text{stat.}) \pm 0.057(\text{sys.})\text{GeV} \quad (4)$$

Then using the value from LEP for $\Gamma(Z^0 \rightarrow e^+e^-) = 83.7 \pm 0.07 \text{ MeV}$ we get

$$\Gamma(W \rightarrow e\nu)/\Gamma(W) = 0.1100 \pm 0.0036(\text{stat.}) \pm 0.0031(\text{sys.}) \quad (5)$$

This preliminary value is compared to previous measurements and to the Standard Model prediction in Table 1.

Table 1: Comparison of measurements of the W width

Who	Mode	Reference	W width
CDF	e	PRL 64,152 (1990)	$\Gamma(W) = 2.20 \pm 0.16 \text{ GeV}$
CDF	μ	PRL 69,128 (1991)	$\Gamma(W) = 2.21 \pm 0.27 \text{ GeV}$
UA1	μ	Phys. Lett. B253,503 (1991)	$\Gamma(W) = 2.19 \pm 0.30 \text{ GeV}$
UA2	e	Phys. Lett. B276,365 (1991)	$\Gamma(W) = 2.10 \pm 0.16 \text{ GeV}$
CDF	e	Preliminary 1993	$\Gamma(W) = 2.033 \pm 0.09 \text{ GeV}$
St. Mod.	e, μ	Ref. [16]	$\Gamma(W) = 2.067 \pm 0.021 \text{ GeV}$

This measurement of the branching ratio is sensitive to new decay modes of the W, e.g. the W decaying into $t\bar{b}$. Although CDF has set a limit on the top quark mass of $108 \text{ GeV}/c^2$, this limit assumes that the top quark decays via the Standard Model decay modes. If, however, the top decays into some other channel, for example $t \rightarrow H^+b$, the limit from the direct search can be evaded. But provided the W couples to $t\bar{b}$ in the normal fashion the measurement of the branching ratio sets a decay-mode independent limit on the top quark mass.

The predicted dependence of the branching ratio on the top quark mass is shown in Figure 8, where the inverse of the branching ratio, $\Gamma(W)/\Gamma(W \rightarrow e\nu)$ is plotted versus top mass (the inverse has uncertainties that are more Gaussian). Both the $1-\sigma$ and 95% *C.L* limits from our new measurement are plotted. The result is a decay-mode independent limit on the top mass of $M_{top} > 62 \text{ GeV}/c^2$, 95% *C.L.*

CDF has previously measured these same quantities in the muon channel as well [17]. The present muon analysis is well underway, although at this short interval after the run there is not yet a preliminary number for R. Figure 9 shows the $W^\pm \rightarrow \mu^\pm\nu$ transverse mass distribution for central muons with $p_T > 20 \text{ GeV}/c$ and $E_t > 20 \text{ GeV}$. Figure 10 shows the invariant mass distribution for dimuon events where both muons have $p_T > 20 \text{ GeV}/c$.

How well can we do in the future with this method? The past measurements have been limited largely by the statistics on the number of $Z^0 \rightarrow e^+e^-$ events. Figure 11 shows the contributions to the uncertainty for the 1988-89 analysis and for this present analysis. Also shown is a guess for how well one could do in Run Ib. One can see that theoretical uncertainties such as the dependence on the parton distribution functions (PDF's) will become comparable to the statistical error. However at the same time we will be able to make better measurements of the PDF's through measurements of related quantities such as the W forward-backward asymmetry, low mass Drell-Yan production, and perhaps charm production (to get at the charm contribution).

To make the above argument quantitative it would be very useful to have a table of the derivatives (dependences) of the measured quantities (Drell-Yan, R, W

asymmetry, etc.) versus the theoretical quantities that are uncertain (the $\bar{u}\bar{d}$ ratio, the gluon behavior at low x , the charm PDF, etc.). Then as D0 and CDF make improvements in the measurements the contributions from the PDF uncertainties to the other analyses will be easier to track.

3 The Forward/Backward Charge Asymmetry in W decay

In $\bar{p}p$ collisions at $\sqrt{s} = 1.8 \text{ TeV}$ approximately 85% of the W bosons are produced in valence-valence or valence-sea collisions [18] of the type

$$u + \bar{d} \rightarrow W^+ \quad \bar{u} + d \rightarrow W^- \quad (6)$$

The W^+ is thus boosted on average in the proton direction, and the W^- is boosted on average in the anti-proton direction. This is one source of a forward-backward charge asymmetry.

A second, competing (in sign) source is the V-A decay of the W. The V-A decay gives a lepton distribution of

$$\frac{d\sigma}{d\cos(\theta^*)} = (1 - \cos(\theta^*)) \quad (7)$$

which tosses the lepton backward (i.e. a positron from W^+ decay gets pushed *away* from the proton direction.)

The relative size of these two competing effects in the asymmetry is dependent on the selection cuts, as well as \sqrt{s} . For our cuts, which select electrons at high p_T (and hence preferentially select decays in which the lepton emerges at 90° from the beam directions), and at $\sqrt{s} = 1.8 \text{ TeV}$, the production effect is dominant, and so one sees more positrons in the proton direction. The measurement is in fact not very sensitive as a test of V-A, given the uncertainties in the PDF's.

Figure 12 shows the W transverse mass distributions for both central ($|\eta| < 1.0$) and plug ($1.1 < |\eta| < 2.4$) electrons. Figure 13 shows the fraction of events with the sign of the charge (i.e. e^+ or e^-) of the electron determined by the tracking chamber versus the rapidity of the electron. For this measurement, where the sign is all important, the maximum rapidity is restricted to $|\eta| < 1.7$

Figure 14 shows new preliminary results on the charge asymmetry versus lepton rapidity. In Figure 14a the data from the central electron measurement, the plug electron measurement, and the central muon measurement are shown separately. In Figure 14b the results of the three measurements are combined. We also show the predictions of recent structure functions, and one not-so-recent (MRSE) just to find something that doesn't fit very well. The agreement with MRSD0, for example, is very good.

4 Drell-Yan Production at low x

The results on low mass Drell-Yan production of lepton pairs from the 1988-1989 run have now become final [19]. The interest is that we can reach relatively low values of x while still at fairly large values of Q^2 . For example, since $x_1 x_2 = m^2/s$, at a mass of $m = 10 \text{ GeV}/c^2$ and $s = (1800)^2 \text{ GeV}^2$, a typical value of x is 0.006.

The measured dilepton mass spectrum has three components:

1. Drell-Yan (the signal)
2. Heavy Flavor-Leptons from b and c decay (mostly b's)
3. 'Junk'- Decay-in-flight, misidentified hadrons...

The analysis untangles the three by using ee , $\mu\mu$, and $e\mu$ samples of opposite-sign and same-sign lepton pairs.. Component 1, 'Junk', is measured to be sign-symmetric. Component 2, 'Heavy Flavor', contributes to $e\mu$ only. We thus subtract the same sign from the opposite sign pairs, getting rid of the 'Junk' contribution, and then subtract off the same-sign subtracted $e\mu$ pairs to get rid of the heavy flavor contribution. The reader is directed to Ref [19] for details.

Figure 15 shows the dilepton invariant mass spectrum $d^2\sigma/dMdy$ in pb per GeV versus the invariant mass of the lepton pair. One sees the falling Drell-Yan spectrum, and the prominent peak at the Z.

The quantity $d^2\sigma/dMdy$ has dimensions of $1/M^3$, and so M^3 times $d^2\sigma/dMdy$ should be flat except for scale-breaking. This quantity is shown in Figure 16, along with predictions using recent parton distributions.

We conclude that the more recent parton distributions are in better agreement with the measured numbers, which sit a little higher than than the old predictions. The measurements can be improved with the new data that we have collected, but this is a hard measurement, as the cross-sections are small. and the trigger thresholds need to be well understood to calculate the efficiency.

5 The W Mass Measurement

For a naive experimentalist like myself, testing the consistency of the electroweak sector of the Standard Model largely reduces to a counting of parameters and of measured quantities. At tree-level the model has three parameters that determine the W and Z masses. Ignoring radiative corrections, both masses are proportional to the vacuum expectation value of the Higgs field $\langle v \rangle$:

$$M_W = \frac{1}{2}g \langle v \rangle \quad (8)$$

and

$$M_Z = \frac{1}{2}\sqrt{g^2 + g'^2} \langle v \rangle, \quad (9)$$

where g is the coupling constant of the $SU(2)_L$ isotriplet bosons $W^{+,-,0}$ to the left-handed weak currents and g' is the coupling for the $U(1)$ of the isosinglet B to the hypercharge current.

Radiative corrections change these predictions for the W and Z masses. The top mass enters (quadratically) through a self-energy loop diagram for the W where the W couples to a virtual $t\bar{b}$ pair. The Z has a similar diagram for a $t\bar{t}$. The contributions of these diagrams increase with top mass as m_t^2/m_W^2 . One can thus put an upper limit on the top mass from a comparison of θ_W measured from the W and Z masses and from low energy determinations of the couplings from measurements of neutrino scattering, α , and G_{Fermi} , or measurements of the g and g' couplings directly from the properties of the Z . A similar limit applies to new heavy generations of quarks provided the 'top' and 'bottom' quarks are very different in mass as in the top and bottom cases. The Higgs mass contributes to the W and Z masses through loop corrections as well, but logarithmically.

There are thus 5 electroweak parameters that dominate the observed masses and couplings: g , g' , $\langle v \rangle$, M_{top} , and M_{Higgs} . There are three related electroweak quantities that are precisely measured, α , G_F , and M_Z . The precise measurement of two more, e.g. M_W and M_{top} to pick two that are accessible to the Collider and which are not degenerate with the others, would fully constrain the model and therefore predict M_{Higgs} . Figure 17 shows the allowed region in the M_W - M_{top} plane from the LEP Z mass constraint [20]. Also shown are the excluded region derived from the CDF limit on the top mass [21], and the $1-\sigma$ limits on the W mass from UA2 and CDF[7].

The dependence on the Higgs mass is logarithmic, and hence hard to measure. For a top mass around 160 GeV, for example, changing the Higgs mass from 100 to 1000 GeV results in a change of 20 GeV in the predicted top mass (holding the W mass fixed), and a change of about 125 MeV in the predicted W mass (holding the top mass fixed). One should note that measuring the top mass to better than this range may be easier than a similar measurement for the W mass.

At present the W mass is known to 270 MeV from the measurement of $M_W = 80.35 \pm 0.37$ GeV by UA2 and the measurement of $M_W = 79.91 \pm 0.39$ GeV by CDF[7]. The world average is then $M_W = 80.14 \pm 0.27$ GeV

The analysis of the data from the 1992-93 run is well underway. There is approximately 5 times the data as from the 1988-89 run. The detailed calibration of the detector, which is one of the crucial ingredients of the measurement, is close to completion. The calibration of the electromagnetic calorimeter is done *in situ* using the measured momentum of electrons above 9 GeV to balance the electromagnetic towers of the calorimeter, and using the momentum of electrons from W decay for the overall calibration. We are thus using the magnetic spectrometer to calibrate the calorimeter in an absolute fashion. Figure 18 shows the spectrum in E/p , where E is the calorimeter response and p is the measured momentum from the track, for electrons from W decay. Also shown is the prediction from a Monte Carlo that

includes radiation. The radiative tail matches the data well. Figure 19 shows the reconstructed Z peak and the Monte Carlo prediction. I would like to emphasize that the Z mass peak is **not** used in the normalization of the W mass, but is used only as a check; this is thus not a measurement of M_W over M_Z , but of M_W . As long as CDF is in this regime where the statistics dominate both the statistical and systematic errors we do better with the direct measurement than by normalizing to the Z mass due to the limited statistics on the Z.

How well will we be able to do on the W mass measurement in the future? The previous CDF measurements were statistics limited, in that the systematic uncertainty was itself limited by the statistics. For example, the measurement of the mean $u_{parallel}$, the component along the lepton direction of the transverse energy recoiling against the W, improves as the root of the number of events. Because the transverse mass of the W is approximated (for $u_{parallel}/Pt_W \ll 1$) by

$$M_T = 2P_T^{lepton} + u_{parallel}, \quad (10)$$

the statistical uncertainty on determining the center of the $u_{parallel}$ distribution enters directly into the systematic uncertainty on the mass.

We are at present therefore in the regime where the overall uncertainty on the W mass scales approximately as the square root of the number of events. One can thus define a figure of merit for a given detector that characterizes the power of the measurement. One such (crude- not all events have equal weight in the mass measurement) figure of merit is the number of W events per pb^{-1} used in the measurement. Another measure is statistical error times the square root of the number of events: this characterizes the power per event. Finally, the statistical error times the square root of the integrated luminosity characterizes both the acceptance (and in the case of UA2, the production cross-section) and the resolution. Table 2 shows these measures for both the published UA2 and CDF measurements, and shows the number of events that have been presented in preliminary fashion by D0 and CDF for the new data. The last entries are very recent, and consequently there are many blanks to be filled in.

At present all uncertainties in the CDF measurement are still scaling approximately with the inverse of the square root of the luminosity (i.e. statistics). Figure 20 shows the uncertainty on the W mass *if* this dependence continues. Figure 21 shows the breakdown of the uncertainties from the 1988-89 analysis. The big contributions to the systematic uncertainty are in the categories of Parallel Balance and Resolution and W Pt, each of which is measured from the data, and whose contributions will decrease with statistics. After Run Ib, for which the goal is $75 pb^{-1}$, if no new systematic uncertainties appear one could hope for an overall uncertainty on M_W of close to 100 MeV. Below this level the ultimate sensitivity is unknown: the number of 50 MeV is bandied about, but cannot yet be taken seriously as either possible or impossible. However if both D0 and CDF could reach the 50 MeV level with $1 fb^{-1}$, the combined number from Fermilab would reach 35 MeV. One can compare this

Table 2: Comparison of existing measurements of the W mass

Who	l	L pb^{-1}	Evts	σ_{stat} MeV	σ_{sys} MeV	σ_{tot} MeV	$\sigma_{stat} \times \sqrt{L}$ MeV/ $(pb)^{-1/2}$	$\sigma_{stat} \times \sqrt{Ev}$ GeV	Ev/pb^{-1} $/pb^{-1}$
CDF	e	4.4	1130	350	240	465	692	11.8 ± 0.4	257
CDF	μ	3.9	592	530	315	620	1046	12.9 ± 0.5	152
UA2	e	13.0	2065	330	170	370	1190	15.0 ± 0.3	159
1992-1993 Results									
D0	e	14.8	8182						553
CDF	e	19	6974						367
CDF	μ	21	5650						269

with projections for LEP200 assuming a beam energy of 88 GeV and an integrated luminosity of $500 pb^{-1}$, which could occur in 1998 after 3 years of running [22]. From direct reconstruction LEP estimates an uncertainty per experiment of 55 MeV, from the excitation curve an uncertainty of 100 MeV, and from the lepton end-point an uncertainty of 150 MeV. Combining all four LEP experiments and a lot of optimism they estimate the direct reconstruction could give a statistical error of 28 MeV and a systematic error of 24 MeV. One really doesn't know what systematic problems one will run into at these levels at D0 and CDF, and the only conclusion I can draw is that at least on paper Fermilab and LEP200 are competitive.

6 $W\gamma$ and $Z^0\gamma$ Production

The production of a heavy vector boson and a photon is of interest because the photon can come from the quark, lepton, and boson lines, and all three of these contributions to the amplitude are needed for gauge invariance. One is thus testing the couplings of the W and the Z to the photon. Figure 22 shows the relevant terms, and defines the couplings κ and λ . These are linearly related to the electric and magnetic dipole moments and quadrupole moments as shown in Figure 22.

Figure 23 is a tabulation of the results from the 1988-89 run on $W\gamma$ and $Z^0\gamma$ production (analysis of the 1992-93 data is underway). The analysis asks for a photon with $E_T > 5 GeV$ separated in $\eta - \phi$ space from the electrons or muons by $\Delta R(\gamma, lepton) > 0.7$. The process is observed in all four modes, and is consistent with predictions[24], albeit with limited statistics. For example, eight events are observed in the $\gamma + W \rightarrow e\nu$ mode with an estimated background of 3.8 events. The net signal of 4.2 ± 3.3 is consistent with the prediction of 4.6 ± 0.4 events. Figure 24 is a summary of the measured values for the parameters and the moments. Figure 25 shows the contours in the plane of the W magnetic moment versus the quadrupole moment derived from this measurement. With the factor of five more data we have

accumulated in the run that has just ended the uncertainties will be decreased significantly, although this is a measurement that is just entering the era of sufficient integrated luminosity to be interesting.

7 WW and WZ Pair Production

The production of WW and WZ pairs tests the gauge couplings as well, although the cross-sections are smaller, and in the most obvious analyses one pays the price for leptonic branching ratios that don't exist in the $W\gamma$ and $Z^0\gamma$ case. Figure 26 reproduces a table from Barger *et al.* [25] that gives the predicted cross-sections for boson pair production. Note that the numbers (in pb^{-1}) are small, and do not include branching ratios. However such events are quite striking. Figure 27 shows a CDF event with three high-Pt electrons and missing Et. Two of the electrons make a system with the invariant mass of the Z, and the third when combined with the missing Et gives the transverse mass of the W. The event is 'typical', in that it is the only such one we have. We hope for many more in the upcoming runs.

8 Acknowledgements

I would like to thank my many CDF colleagues who worked so hard in the last run. Special thanks to Sacha Kopp and Greg Sullivan for providing figures for the R analysis in electrons, Bill Badgett and Mark Krasberg for figures for the R analysis in muons, Mark Dixon for figures for the forward/backward W asymmetry, Steve Errede for the $W\gamma$ plots, David Saltzberg for enduring the pain of getting W mass plots blessed, and Sarah Eno and Jimmy Proudfoot for their efforts as the CDF electroweak convenors in getting out these results so rapidly after the run. I thank Jon Rosner and James Stirling for guidance and help. Lastly, I would like to thank the conference organizers for providing such a well-organized and thoughtful conference.

References

- [1] The luminosity numbers quoted here have an uncertainty of approximately 10%. The new CDF measurement of the total cross-section carries the implication that all luminosities may have to be lowered by approximately 10%, and all cross-sections will have to be raised by the same amount (the quoted uncertainty in the luminosity has been 7%).
- [2] The number plotted is the integrated luminosity used in published analyses, i.e. it is neither the complete running total nor the luminosity per year, but the effective luminosity seen by published results. The difference is in most cases minor as the curve is rising rapidly.

- [3] UA2 Collaboration, J. Alitti et al., Z. Phys. C47,11 (1990)
- [4] CDF Collaboration, F. Abe et al., Phys. Rev. D44,29 (1991)
- [5] A.D.Martin, W.J.Stirling, R.G.Roberts RAL-93-027, Apr. 1993; also Phys.Lett.B306:145-150,1993; ERRATUM-ibid.B309:492,1993.
- [6] G. Altarelli, R. K. Ellis, and G. Martinelli, Z. Phys. C27:617,1985.
- [7] CDF Collaboration, F. Abe et al., Phys. Rev. Lett. 65, 2243 (1990), Phys. Rev. D43, 2070 (1991);UA2 Collaboration, J. Alitti et. al., Phys. Lett. B276,354 (1992)
- [8] N. Cabibbo,Third Topical Workshop on Proton-Antiproton Collider Physics, Rome, 12 Jan, 1983, pp. 567-569.
- [9] F. Halzen and M. Mursula, Phys. Rev. Lett. 51, 857 (1983).
- [10] CDF Collaboration, F. Abe et al., Phys. Rev. D44,29 (1991), Phys. Rev. Lett. 64, 152 (1990)
- [11] The E/p cut has been changed [4] from $E/p < 1.5$ to $0.5 < E/p < 2.0$, and the cut on the chisquared on the shower maximum (strip) chamber has been changed from 15. to 10.
- [12] The central electromagnetic calorimeter fiducial region covers a rapidity range from 0. to 1.0, the plug from 1.1 to 2.4, and the forward calorimeter from 2.4 to 4.2.
- [13] A.D.Martin, R.G.Roberts, and W.J.Stirling, Phys. Lett. 228B,149(1989), and W.J. Stirling, private communication.
- [14] S. Kopp, private communication.
- [15] L. Rolandi, in Proceedings of the XXVI Int. Conf. on High Energy Physics, Aug. 1992, Dallas Texas, p.56, James R. Sanford, ed., AIP Conf Proc.272
- [16] J. Rosner, M. Worah, and T. Takeuchi, Univ. of Chicago preprint EFI 93-40, Aug. 1993
- [17] CDF Collaboration, F. Abe et. al, PRL 69,128 (1991)
- [18] See, for example, F. Halzen and S. Keller, in Proceedings of the Workshop on Hadron Structure Functions and Parton Distributions, FNAL, April 1990, D. Geesaman, J. Morfin, C. Sazama, and W.K. Tung, eds. (World Scientific).
- [19] F. Abe et. al, FERMILAB-PUB-93/133-E, submitted to Phys. Rev. D., May 1993.

- [20] I thank Chris Quigg, Chris Hill, and Jon Rosner for this figure.
- [21] Teruki Kamon, for the CDF collaboration, these proceedings.
- [22] Minutes of a LEPC meeting. spring 1993.
- [23] Srini Rajogopalan, for the D0 collaboration, these proceedings.
- [24] The numbers of predicted events are derived from the Monte Carlo of U. Baur interfaced to the CDF simulation. Also see U. Baur and E.L. Berger, Phys. Rev. D41,1476 (1990), and Phys.Rev.D47, 1993.
- [25] V. Barger, T.Han, J.Ohnemus, and D.Zeppenfeld, PRD41,2782 (1990)

CDF—Run Ia (1992-1993)

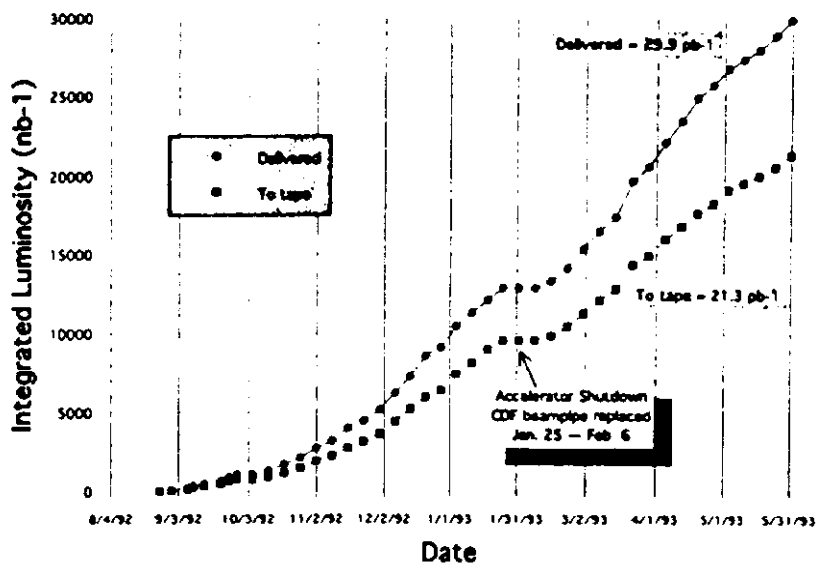


Fig.1 Integrated luminosity versus time for Run Ia.

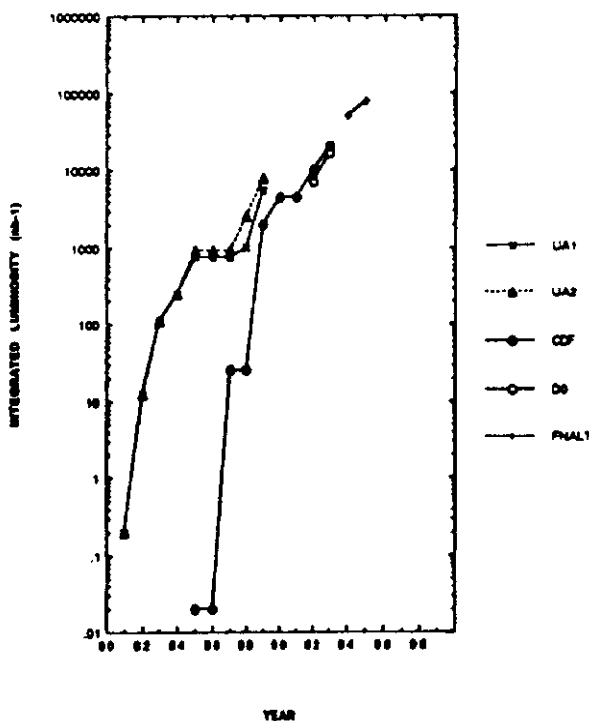


Fig.2 A history of the integrated luminosity per dataset versus year. Note that the last two points are only projections.

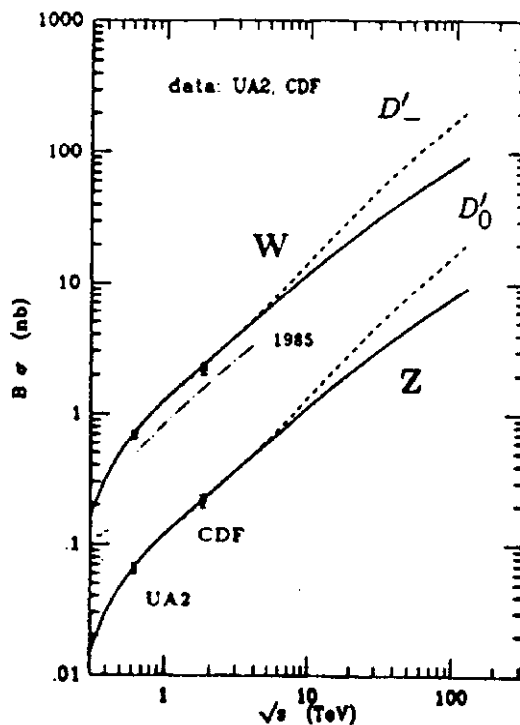


Fig.3 The cross-sections as measured by CDF in 1988-1989 [4] and UA2 [3].

**CDF Preliminary for
18.4 pb⁻¹ of 1992-1993 Run
Summary of Results for R:**

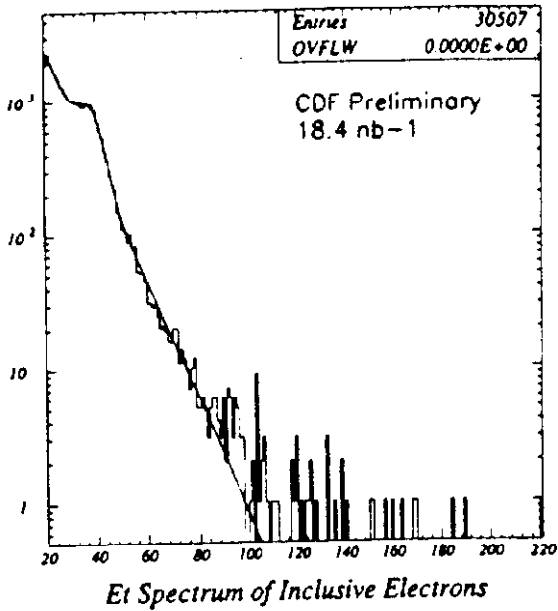


Fig.4 The E_T spectrum of inclusive electrons. Note the Jacobian peak of the W and Z.

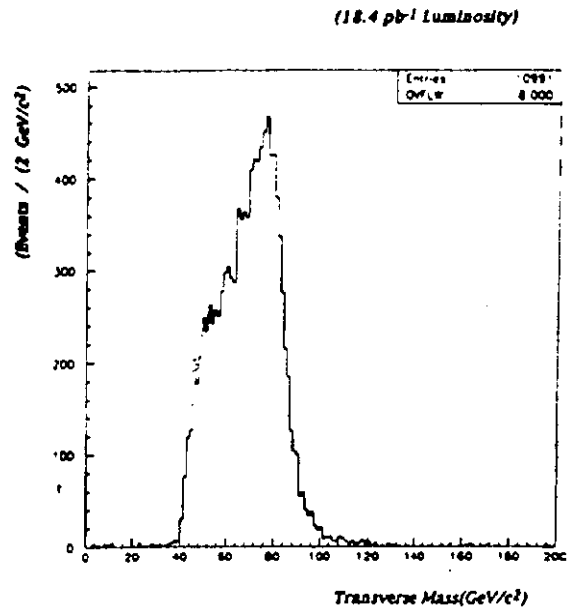


Fig.5 The transverse mass spectrum for inclusive electrons that have E_T greater than 20 GeV.

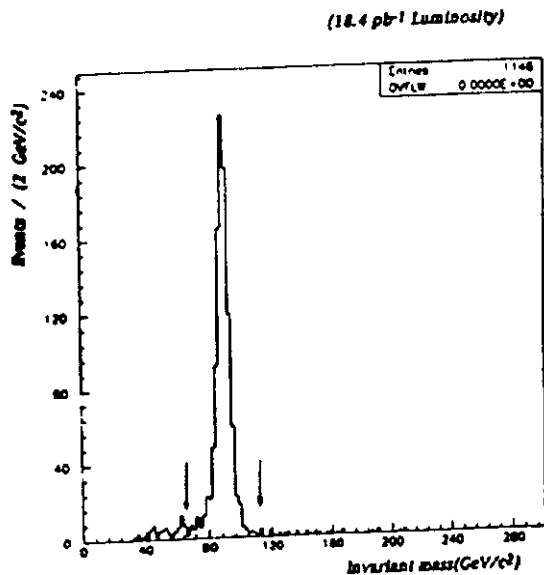


Fig.6 The invariant mass spectrum for inclusive electrons that also have a second electromagnetic isolated cluster. The arrows identify the cuts used to select Z candidates.

	W's	Z's
Candidates:	10991	1053
Background:	1175 ⁺¹²¹ _{-.99}	52 ± 9
Signal:	9816 ± 105 ± 106	1001 ± 32 ± 9
Acceptance		
<i>A_{w,z}</i>	0.338 ± 0.006	0.372 ± 0.006
<i>A_w/A_z</i>	0.908 ± 0.015	
Efficiencies		
<i>ε_{w,z}</i>	0.749 ± 0.013	0.731 ± 0.015
<i>ε_w/ε_z</i>	1.025 ± 0.012	
Drell-Yan Correction		1.01 ± 0.01
<i>σ(W→eν)</i> <i>σ(Z→ee)</i>	10.65 ± 0.36 (stat.) ± 0.27 (sys.)	

Fig.7 A table of the acceptance, efficiencies, background, and signal for the W and Z cross-section ratio measurement in the electron modes.

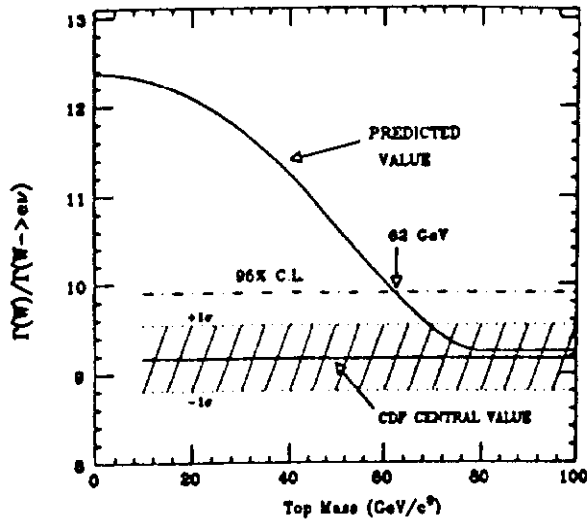


Fig.8 The predicted dependence of the inverse of the branching ratio, $\Gamma(W)/\Gamma(W \rightarrow e\nu)$, as a function of top mass. The new preliminary results from CDF are shown, with both the 68% and 95% confidence limits. The resulting limit on the the top mass is $M_{top} > 62 \text{ GeV}/c^2$, 95% C.L..

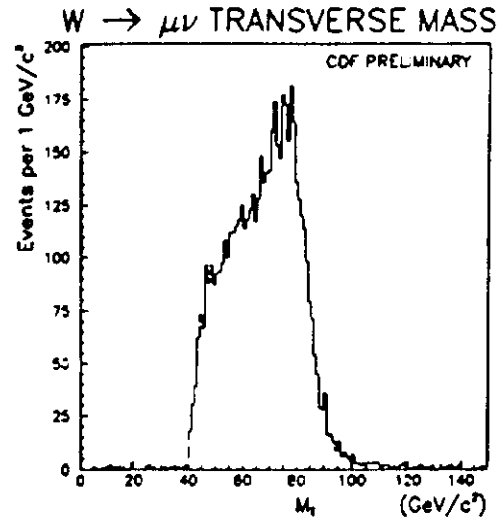


Fig.9 The $W^\pm \rightarrow \mu^\pm \nu$ transverse mass distribution for central muons with $p_T > 20 \text{ GeV}/c$ and $E_T > 20 \text{ GeV}$.

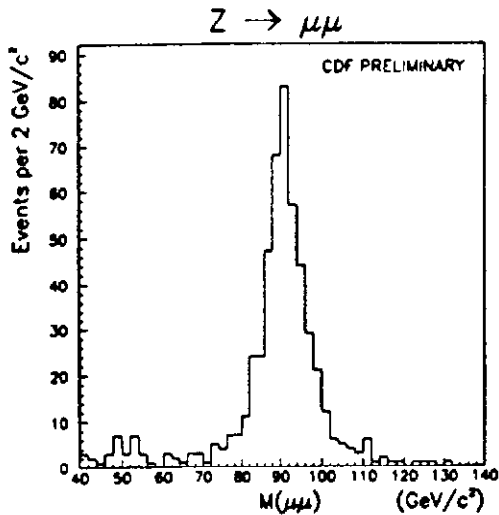


Fig.10 The invariant mass distribution for dimuon events where both muons have $p_T > 20 \text{ GeV}/c$.

Prospects for the
Uncertainty in $\Gamma(W)$

Source of Uncertainty	1988 Run (4.4 pb ⁻¹)	1992 Run (18 pb ⁻¹)	1994 Run (100 pb ⁻¹)
Statistics	7.0 %	3.1 %	1.4 %
Boson ID	2.9 %	1.2 %	> 1 %
Efficiencies			
Background Subtraction	0.1 %	0.7 %	0.5 %
Acceptances			
- $M_{\mu\nu}$	0.8 %	0.4 %	-
-Detector Model	2.9 %	0.9 %	0.6 %
-PDF's	3.0 %	1.5 %	0.6 % 77
Drell-Yan Estimate	1 %	1%	0.5 %
Total B	6.8 %	4.2 %	2.0 %
Uncertainty			
$\alpha(W)/\alpha(Z)$ Theory	1 %	1 %	0.5 %
LEP $\Gamma(Z)$	3 %	0.3 %	0.2 %
Total $\Gamma(W)$ Uncertainty	9.4 %	4.4 %	2.1 % 77

Fig.11 The contributions to the uncertainty for the 1988-89 analysis and for this present analysis. Also shown is a guess for how well one could do in Run Ib.

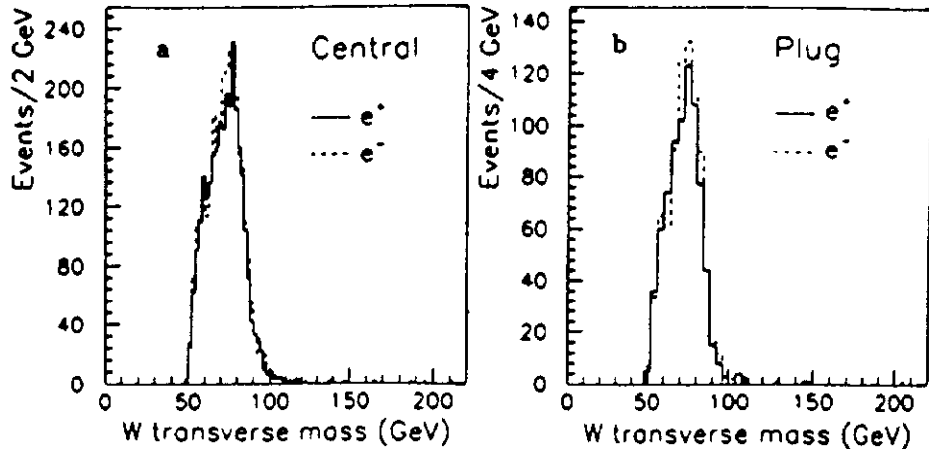


Fig.12 The W transverse mass distributions for a) central ($|\eta| < 1.0$) and b) plug electrons ($1.1 < |\eta| < 2.4$).

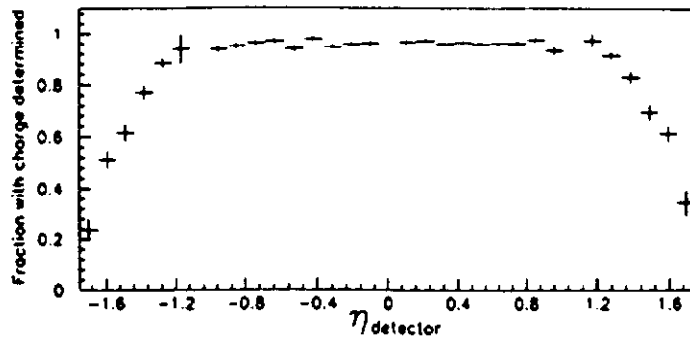


Fig.13 The fraction of events with the sign of the charge (i.e. e^+ or e^-) of the electron determined by the tracking chamber versus the rapidity of the electron.

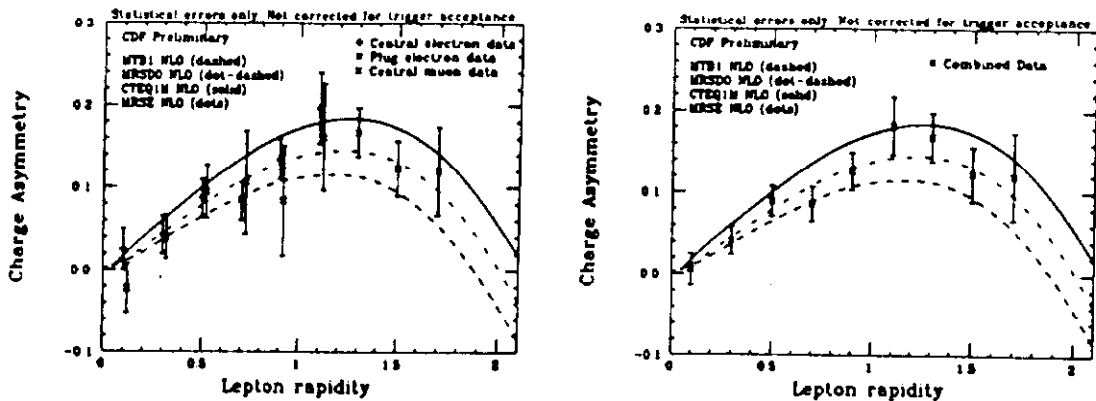


Fig.14 a) The charge asymmetry versus lepton rapidity from the central electron measurement, the plug electron measurement, and the central muon measurement. b) The combined results of the three measurements.

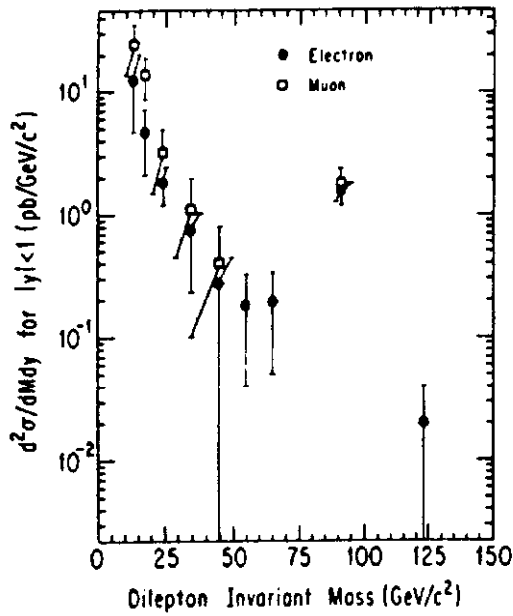


Fig.15 The dilepton invariant mass spectrum $d^2\sigma/dMdy$ in pb per GeV versus the invariant mass of the lepton pair. One sees the falling Drell-Yan continuum spectrum, and the prominent Z peak.

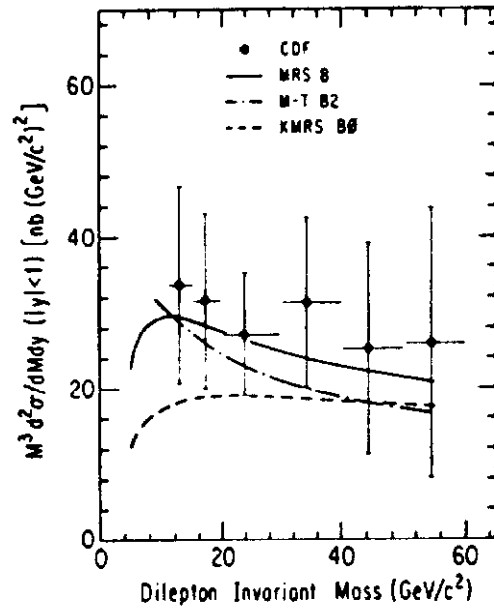


Fig.16 The dilepton invariant mass spectrum $d^2\sigma/dMdy$ multiplied by the mass cubed versus the mass of the lepton pair. The curves are predictions of recent parton distribution functions.

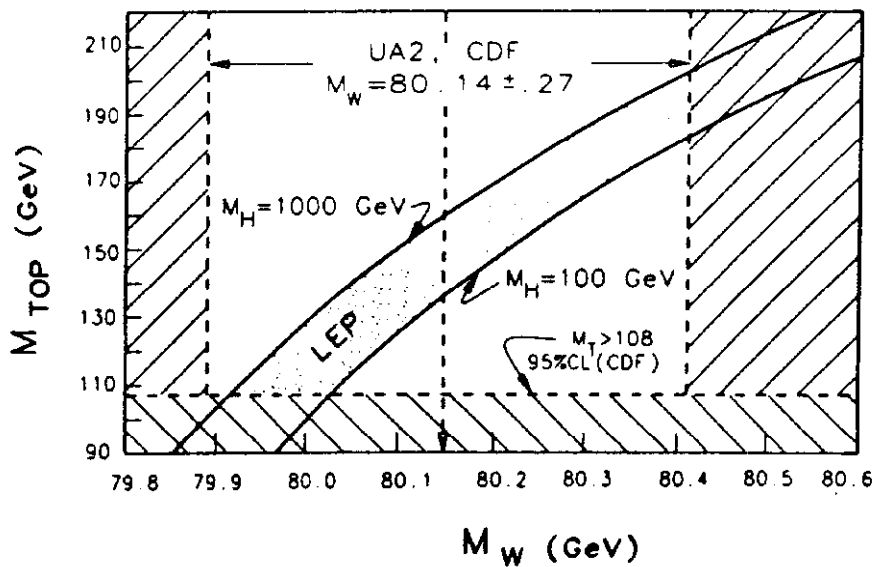


Fig.17 The allowed region in the M_{top} - M_W plane assuming the Standard Model, after Ref[20]

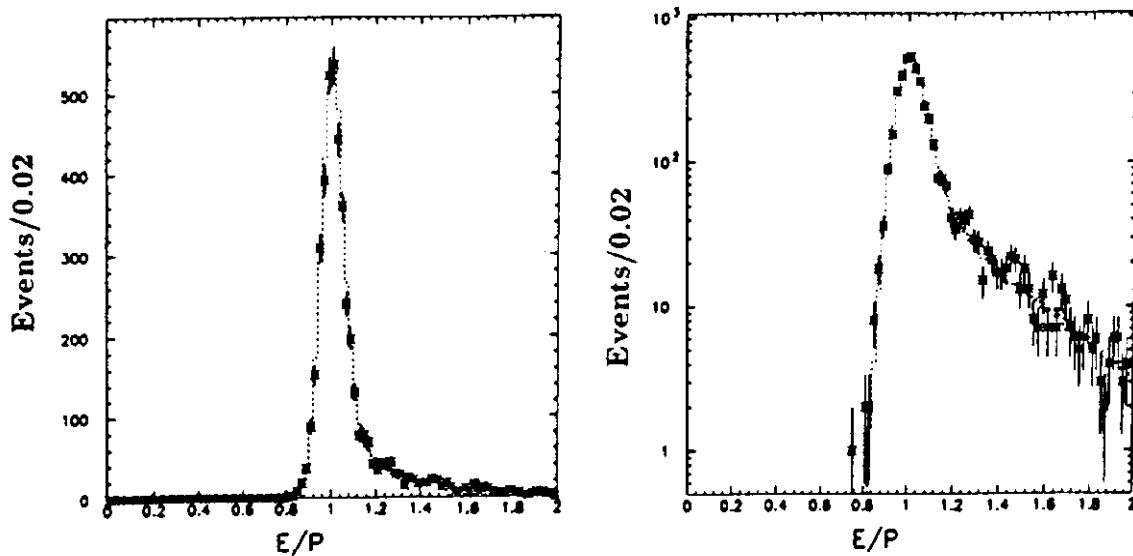


Fig.18 The 1992-1993 data on E/p , where E is the calorimeter energy and p is the track momentum, for electrons from W decay on a) a linear plot, and b) a log plot. The curve is the prediction of a radiative Monte Carlo. Note the good agreement. This is the calibration for the electron in the W mass measurement.

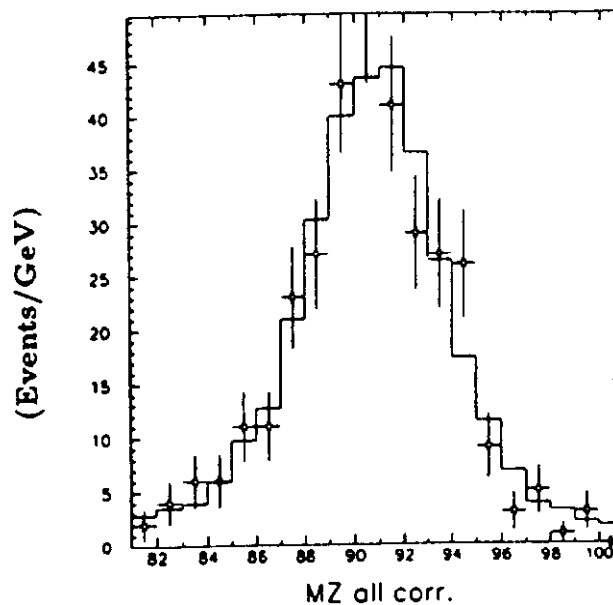


Fig.19 The measured Z mass spectrum in dielectron decays. The normalization is determined from E/p (see Fig. 18), and is absolute. The histogram is the prediction of the Monte Carlo. The Z mass serves as a check on the normalization, but is not used.

IF (!!) the Uncertainty scales as Statistics

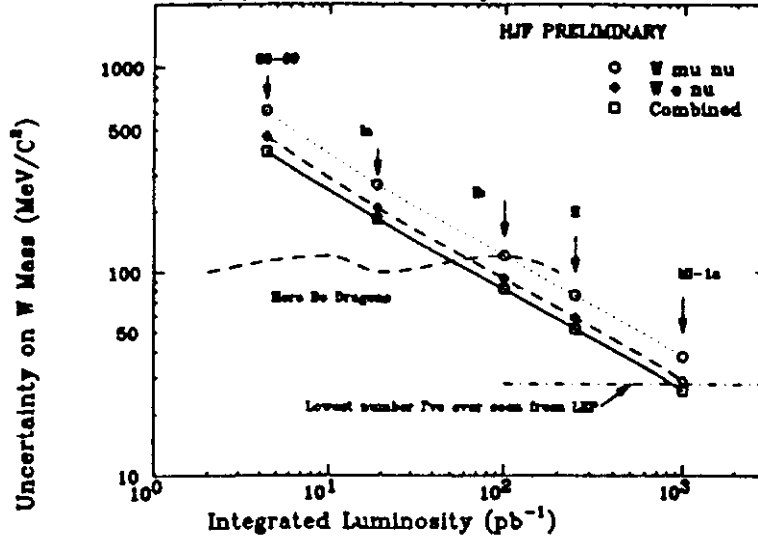


Fig.20 An extrapolation of the uncertainty on the W mass, from the CDF electron, muon, and combined analyses, versus integrated luminosity, (naively) assuming that the systematic uncertainties continue scaling with statistics.

TABLE III. Uncertainties in the W mass measurement. All uncertainties are quoted in units of MeV/c². In parentheses are the statistical (and overall) mass uncertainties if F_W is determined in the fit as well. The scale uncertainties are in common with the Z mass measurement (Ref. 6). The uncertainties which are the same for both samples are listed as common.

Uncertainty	Electrons	Muons	Common
Statistical	350 (440)	530 (650)	
Energy scale	190	80	80
(1) Tracking chamber	80	80	80
(2) Calorimeter	175		
Systematics	240	315	150
(1) Proton structure	60	60	60
(2) Resolution, W _{PT}	145	150	130
(3) Parallel balance	170	240	
(4) Background	30	110	
(5) Fitting	30	30	30
Overall	465 (540)	620 (725)	

Fig.21 The breakdown of the contributions to the CDF Wmass measurement in the 1988-89 analysis.

$$L_{WW} = -ie \left[(W_{\mu\nu}^\dagger W_{\mu\nu} A^\nu - W_{e\nu}^\dagger A_\nu W_{e\nu}) + \kappa W_{\mu\nu}^\dagger W_{\nu e} F^{\mu\nu} + \frac{\lambda}{M_W} W_{\lambda\mu}^\dagger W_{\nu e} F^{\mu\nu} + \kappa' W_{\mu\nu}^\dagger W_{\nu e} F^{\mu\nu} + \frac{\lambda'}{M_W} W_{\lambda\mu}^\dagger W_{\nu e} F^{\mu\nu} \right]$$

$$F_{\mu\nu} = \partial_\mu A_\nu - \partial_\nu A_\mu, F'_{\mu\nu} = \frac{1}{2} \epsilon_{\mu\nu\alpha\beta} F^{\alpha\beta}, W_{\mu\nu} = \partial_\mu W_\nu - \partial_\nu W_\mu$$

$$\begin{aligned} \mu_W &= \frac{e}{2M_W} (1 + \kappa + \lambda) && \text{Magnetic Dipole Moment} \\ Q_W &= -\frac{e}{M_W} (\kappa - \lambda) && \text{Electric Quadrupole Moment} \\ d_W &= \frac{e}{2M_W} (\kappa' + \lambda') && \text{Electric Dipole Moment} \\ Q'_W &= -\frac{e}{M_W} (\kappa' - \lambda') && \text{Magnetic Quadrupole Moment} \\ \langle r^2 \rangle &= \frac{e}{M_W^2} (\kappa + \lambda) && \text{Mean-Squared Charge Radius} \end{aligned}$$

$$\begin{aligned} \mu_W^{\text{SM}} &= \frac{e\hbar c}{2M_W} = 3.691 \pm 0.012 \times 10^{-16} \text{ MeV/T} \\ \mu_e^{\text{SM}} &= \frac{e\hbar c}{2M_e} = 5.788 \pm 0.000 \times 10^{-11} \text{ MeV/T} \\ Q_W^{\text{SM}} &= -e \left(\frac{\hbar c}{M_W^2} \right) = -e\lambda_W = 6.063 \pm 0.041 \times 10^{-4} \text{ e-fm}^2 \\ \lambda_W &= \frac{e\hbar c}{M_W^2} = 2.462 \pm 0.008 \times 10^{-3} \text{ fm} \end{aligned}$$

Fig.22 The definition of the parameters κ and λ, and the relationship of the the W and Z dipole and quadrupole moments to them. Also given are the expected numerical values in the Standard Model.

Channel	N_{obs}	ΣN_{signal}	N_{signal}	$N_{SM}^{W\gamma}$
$e W \gamma$	8	$3.8 \pm 0.8 \pm 1.5$	$4.2 \pm 2.9 \pm 1.5$	4.6 ± 0.4
$\mu W \gamma$	5	$2.2 \pm 0.4 \pm 0.9$	$2.6 \pm 2.3 \pm 0.9$	2.5 ± 0.2
$e Z \gamma$	2	$0.3 \pm 0.1 \pm 0.1$	$1.7 \pm 1.4 \pm 0.1$	1.2 ± 0.1
$\mu Z \gamma$	2	$0.1 \pm 0.1 \pm 0.1$	$1.9 \pm 1.4 \pm 0.1$	0.7 ± 0.1

Fig.23 A summary of the number of measured and expected events from the 1988-89 data for the $W\gamma$ and $Z^0\gamma$ analysis.

Parameter	CL Range	$e + \mu$ Limits
$\Delta\kappa$ ($\lambda = 0$)	68.3% DS CL	$0.0^{+0.3}_{-0.3}(stat) \pm 0.6(syst) = 0.0^{+0.3}_{-0.3}(stat - syst)$
	68.3% SS CL	$-3.2 < \Delta\kappa < +3.7$
	90.0% SS CL	$-5.7 < \Delta\kappa < +6.1$
	95.0% SS CL	$-6.5 < \Delta\kappa < +7.0$
λ ($\Delta\kappa = 0$)	68.3% DS CL	$0.0^{+0.3}_{-0.3}(stat) \pm 0.3(syst) = 0.0^{+0.3}_{-0.3}(stat - syst)$
	68.3% SS CL	$-1.6 < \lambda < +1.6$
	90.0% SS CL	$-2.7 < \lambda < +2.7$
	95.0% SS CL	$-3.1 < \lambda < +3.1$

Fig.24 A summary of the measured values and limits on the parameters κ and λ from the 1988-89 data.

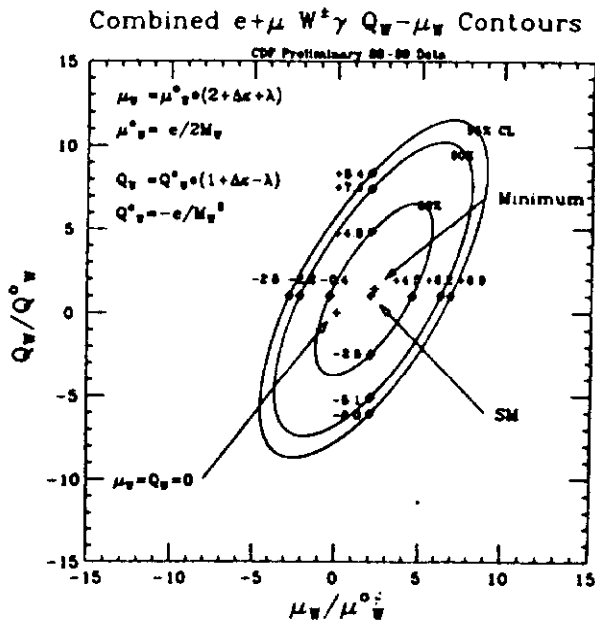


Fig.25 The derived values and limits on the W quadrupole and dipole moments from the 1988-89 data

$\sqrt{s} = 1.8 \text{ TeV}$	$n=0$	$n=1$	$n=2$
$\gamma\gamma$	11	5	2.6
$\gamma W^+ + \gamma W^-$	8.6	2.7	1
γZ	7	2	0.5
W^+W^-	6.7	2.3	0.5
$ZW^+ + ZW^-$	1.7	0.6	0.2
ZZ	0.7	0.3	0.06

Fig.26 The predicted cross-sections [25] in pb^{-1} for boson pair production.

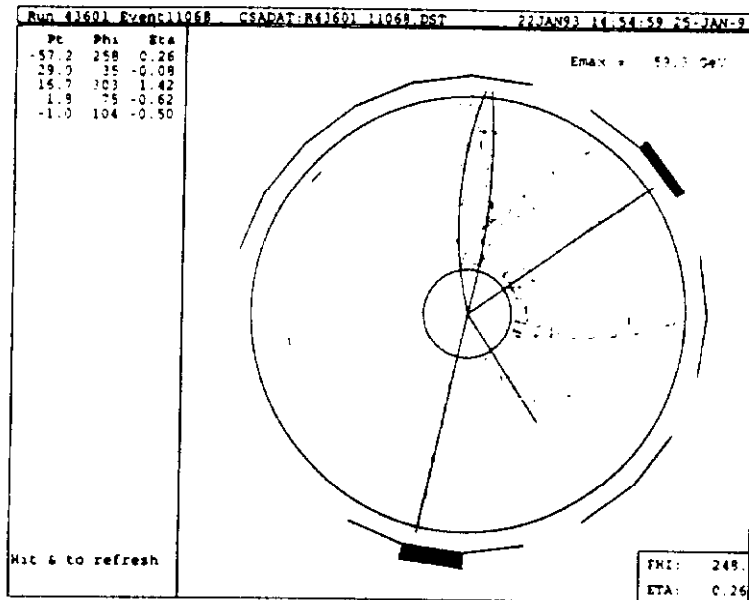
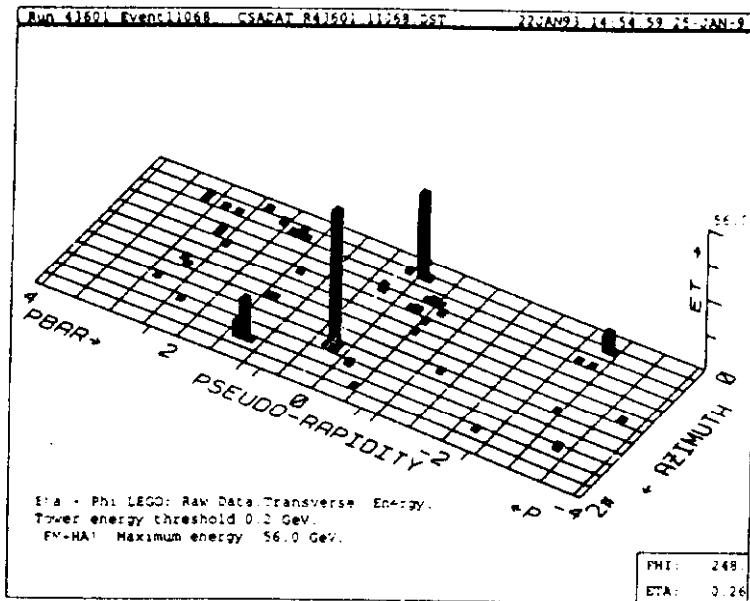


Fig.27 An event with three high-Pt electrons and missing Et. Two of the electrons make a system with the invariant mass of the Z, and the third when combined with the missing Et gives the transverse mass of the W.